SCINTILLATOR DETECTORS FOR THE ESS HIGH ENERGY WIRE SCANNER

B. Cheymol*, European Spallation Source, Lund, Sweden

Abstract

In the ESS linac [1], during commissioning and restart phase, wire scanner (WS) will be used intensively to characterize the transverse beam profiles. At low energy, the mode of detection is based on Secondary Emission (SE), while at energies above 200 MeV, the primary mode of detection will be the measurement of the hadronic shower created in the thin wire.

In this paper we will present the design and the output signal estimation of the shower detector, based of inorganic crystal and silicon photodetector

INTRODUCTION

In the ESS superconducting linac and downstream, 8 WS stations will be installed alone the beam line. Each station will be equipped with two linear actuator to sample the separately the transverse planes and the last 5 stations, in the elliptical sections and in the transfer line to the target, will be used in shower detection mode in addition of the SE signal from the wire. The actuator fork will be equipped with a 40 μm tungsten wire, for the ones to be used in the shower mode, the detectors will be positioned 400 mm downstream the wire [2].

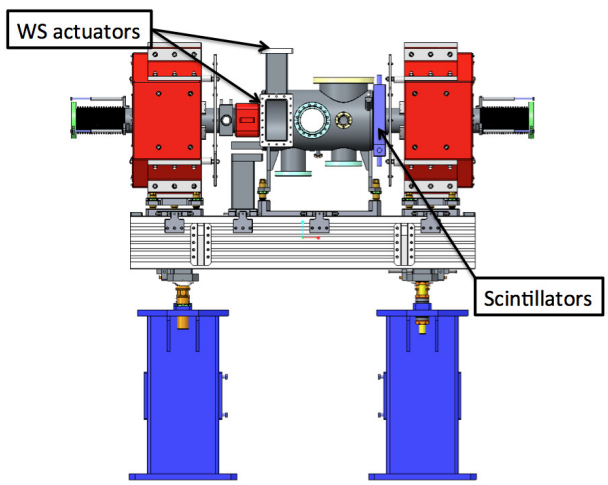

Figure 1: Preliminary design of the elliptical LWU, the total length flange to flange is ≈ 1932 mm, WS actuators are not shown (courtesy of STFC Daresbury Laboratory).

As shown in Fig. 1, due to the low energy of beam compared to proton synchrotron, the full system will be installed in a Linac Warm Unit (LWU), between two quadrupoles. This geometry has been chosen in order to avoid perturbation of the hadronic shower if the detectors would have been installed downstream the quadruple.

* benjamin.cheymol@esss.se

DETECTOR CONCEPT

In high energy physics experiment, wavelength shifting (WLS) fibers are often used to collect the light from scintillator in order to reduce calorimeter geometry complexity [3]. The same approach can be use for the ESS wire scanner, not to simplify the geometry but to protect the photodetector from radiation.

The light generated in the scintillator can be collected through a fiber. which can transport the light to the photodetector installed in an area with less radiation compare to the accelerator tunnel. In an ideal case, the photodetector can be installed in the klystron gallery in the same electronic cabinet as its front end electronic and its digitizer card.

Detector Architecture

The acquisition electronic of the ESS WS is currently under development at Synchrotrone Elettra Trieste. For the SEM mode, it is foreseen to use two separated channels per wire, one with high gain and low bandwidth the other with a low gain and high bandwidth. With this setup it will possible to get a high dynamic range for the profile in a single scan. The same concept will be used for the scintillator readout.

Previous simulations show that 4 separated detector are needed to insure good homogeneity of the signal across the beam pipe [2], each detector will be connected to 2 Front-End (FE) electronic as for the SEM mode. The assembly geometry of the detector is shown in Fig. 2.

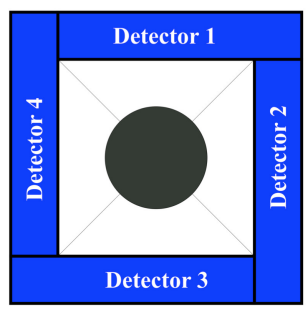

Figure 2: Detector assembly for the ESS WS system.

A combination of WLS fibber and clear fiber will be used to transport the light from the detector to a radiation free area, the detector architecture is shown in Fig. 3.

The scintillation light will be collected by two WLS fiber on each detector assembly, since the attenuation length of this fiber is high (few meters), their lengths have to be kept as short as possible. Silica fiber have a low attenuations, and are better candidates to transport the light over a long distance, for the ESS application the length from the WS station in the tunnel to the electronic rack in the klystron gallery is about 60 meters.

ISBN 978-3-95450-178-6

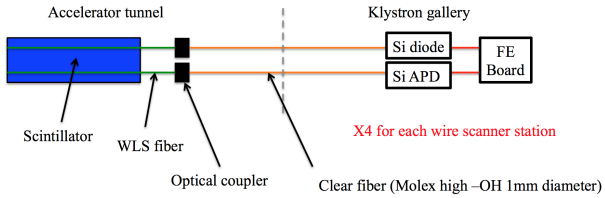

Figure 3: Conceptual design of the ESS wire scanner shower detector.

The light will be converted to current by a photodiode and an avalanche photodiode, in order to increase the dynamic range of the measurement. Each photodetector will be connected to its own FE end electronic.

Scintillator and WLS Choice

Most of the plastic and crystal scintillator have their peak emission in the visible range of the light, more precisely in the blue-green region. WLS can be used to shift the blue light to green light, their absorption peak shall match the peak emission of the scintillator, the BCF-91a from Saint Gobain and the Y-11 from Kuraray have a peak absorption close to 420 nm, which corresponds to the peak emission of the majority of plastic scintillator. Unfortunately, the radiation dose in the accelerator tunnel might be too high for organic scintillator, crystals are less sensitive to radiation and seems a better option.

One alternative to plastic scintillator is to use the LSO scintillator, which had a peak emission at 420 nm, a fast decay time (40 ns) and a high photon yield ($\approx 30\ \gamma\ .\text{keV}^{-1}$), in addition, the LSO is not hydroscopic unlike the NaI crystal. The LSO has been study extensively for calorimetry application for high energy physics and is available from different supplier [4].

As show in Fig. 4 and Fig. 5, its spectra matches the two WLS fibers considered, 80 % of the spectra are absorbed, only the high wavelengths are outside the absorption spectra of the fibers.

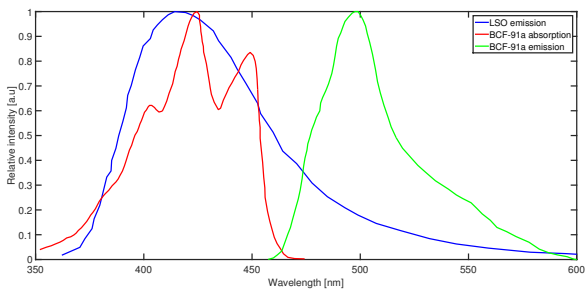

Figure 4: Optical spectra of the Saint Gobain BCF-91A wavelength shifter.

WLS fibers are available on different sizes with single or double cladding, in this study, a 1 mm diameter single clad fiber has been considered in order to match the numerical aperture (NA) of a silica fiber and its diameter. The decay time of such fibers is few ns.

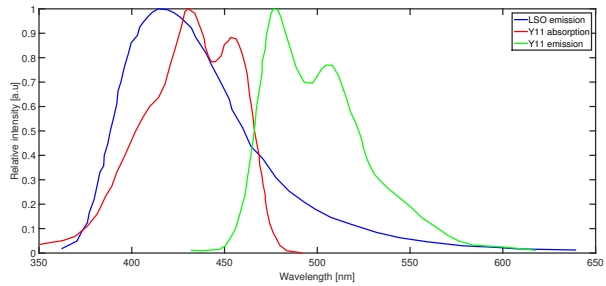

Figure 5: Optical spectra of the Kuraray Y11 wavelength shifter.

SIMULATIONS OF THE DETECTOR

The light production and collection have been simulated by the Monte Carlo (MC) code FLUKA [5], the shifting process, the light transport have been treated analytically in post processing.

The detector assembly geometry used in the MC simulations is shown in Fig 6.

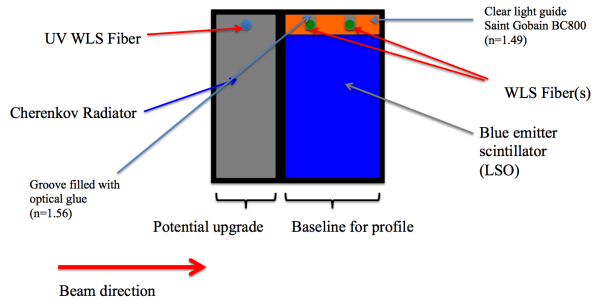

Figure 6: Cross section of the detector assembly used in the MC simulations.

The crystal might be difficult to machine, therefore, a plastic light guide (Saint Gobain BC-800, $n = 1.49$) will be used to installed the WLS fiber in groove filled with optical glue ($n = 1.56$), the detector size is $250 \times 45 \times 30 mm^3$, the light guide dimension is $250 \times 5 \times 30 mm^3$. All the assembly in surrounded by reflecting material, with a reflexion varying index from 0.94 to 0.99 and encapsulated in an aluminum box with a thickness of 2 mm. The WLS fiber has been simulated as a cylinder of 1 mm diameter for the core surrounding with a 20 μm thick clad, materials are polystyrene for the core and PMMA for the clad.

In addition, for an upgrade phase of the WS system, a Cherenkov radiator (in quartz) will be installed in front of the scintillator assembly. Bremsstrahlung background from the cavities might perturb the profile measurement, a Cherenkov detector is insensitive to this radiation and should allow beam profile measurement when the cavities are at their peak accelerating gradient. A similar detector architecture is foreseen for the Cherenkov detector with an UV WLS fiber, simulations is on going at the time this paper is written [6]. Nevertheless, the quartz plate has been implemented

ISBN 978-3-95450-178-6

in the MC simulations in order to simulate the complete hadronic shower generated by the beam interaction with all the material before the scintillator assembly.

Light Collection and Transport

The light production and the absorption by the WLS fiber have been simulated with a simplified geometry. In the MC code, only one scintillator assembly has been simulated with a beam interacting directly with the detector. The number of photons generated in the crystal and the number of photons absorbed in the WLS fiber core have been measured for different reflective material index and separately on both fibers. The results show that light collection yield per fiber varies from 9 % to 14 % as function of the reflective index. The number of photon absorbed in the WLS fiber cores identical for the 2 fibers, thus no effect of detector inhomogeneity is expected.

The conversion in the WLS fiber and the light transport has been calculated in post processing. In the MC code, the scintillation light is monochromatic, a coefficient equal 0.8 has been applied to simulate the non absorption of the high energy wavelength of the LSO spectrum. In addition a the WLS quantum efficiency of the WLS fiber is set at 0.85, and the light trapping efficiency to 0.03.

The last parameter might be increased if the fiber end is wrapped by a reflecting material, in the simulation presented in this paper, it is assumed that the light is not reflected and thus lost. Note that the trapping efficiency can go up to $\approx 0.06 - 0.07$ if the light is fully reflected on the fiber end.

As mentioned previously, the WLS fibers have a short attenuation length, clear plastic fiber have also a short length for our application and are radiation sensitive. Silica fibers have long attenuation length and are less sensitive to radiation, two options have been estimated:

- A pure Silica fiber ($NA \approx 0.22$)
- A silica fiber with hard polymer cladding (SPC) ($NA \approx 0.48$)

Both have attenuation equal to ≈ 25 dB.km^{-1} at the peak emission of the WLS fiber (500 nm). The pure silica fiber has a higher resistance to radiation, but a low NA compare to the WLS fiber ($NA \approx 0.5$), only 40 % of the light from the WLS fiver can be trapped in the silica fiber, in addition the optical connector has an efficiency of 80-90 %, in total the full efficiency of this system is about 30 %.

Due to the higher NA of the SPC fiber, up to 90 % of the light coming from the WLS fiber can be trapped and transport. Nevertheless the radiation resistance of this fiber is less, one possible mitigation is to split the clear fiber path in two. The first one from the detector to the tunnel penetration will allow easy maintenance and replacement of the exposed part of the fiber, the other, from the penetration to the klystron gallery. In this case the fiber will not exposed to high radiation dose and will be installed permanently in the cable tray. Two optical connectors are needed for the solution, assuming he same efficiency of ≈ 85 %, the proportion of the light transported is up to 60 %.

The two options have been considered for the signal estimation.

Signal Estimation

For this simulation, a simplified geometry of the LWU has been modeled in the MC code, the wire consists in a foil with a thickness equal to 32 μm to take in account the round shape of the wire, the energy deposited in each scintillator has been measured and then use as input for post processing. In the first step, the number of photons generated per proton crossing the wire (in the center of the beam pipe) has been estimated for beam energy from 100 MeV to 2100 MeV by converting the deposited energy in photon (see Fig. 7).

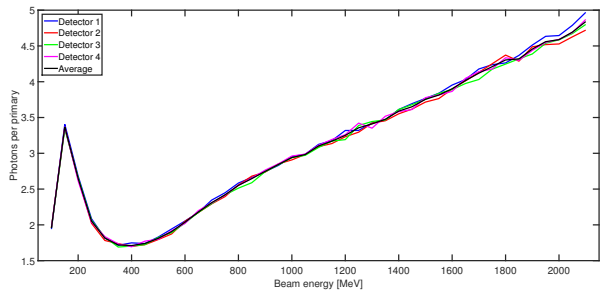

Figure 7: Number of photons generated in the LSO crystals per proton crossing the wire as function of the beam energy.

The response of the 4 scintillators is almost equal, an average value has bee taken for the next steps of the study. The minimum signal is expected for a beam energy equal to 400 MeV, above this energy, the signal increase almost linearly with the beam energy. A peak can be seen at 150 MeV, corresponding to a full energy deposition of scattered proton in the detector.

These data have been then used to estimate the peak light power at 400 and 2000 MeV as function of a clear fiber length for the two options presented in the previous section. In this estimation, the light collection efficiency of the WLS fiber is set to 11 % which correspond to a reflective index of the material equal to 0.96, the emission of the WLS is assumed to be monochromatic with a peak at 500 nm. The beam sizes are assumed to be equal to 2 mm in both transverse planes and the beam intensity is set to 62.5 mA.

As shown in Fig. 8, the light power varies by a factor 5 depending on the beam energy and on the efficiency of the clear fiber. At the ESS facility, it expected to have a fiber length no longer than 60 meters, in this case the peak light power has a range from ≈ 4 W at 400 MeV with lowest fiber efficiency to $\approx$19 W at 2000 MeV and the highest fiber efficiency.

The light power has been converted to current at the exit of a photodiode and of an APD, for this, a preliminary choice of the detector has been done. The photodetectors shall have a high sensitivity at 500 nm, a surface larger than the section of the fiber to insure good optical coupling and a

ISBN 978-3-95450-178-6

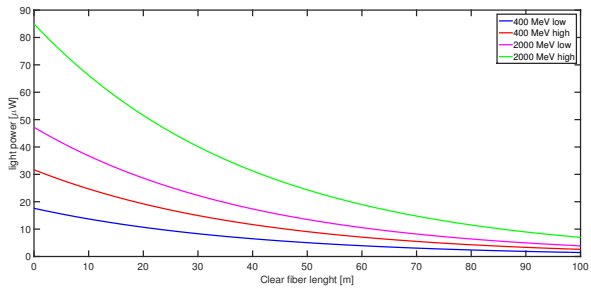

Figure 8: Peak light power as function of the clear fiber length for a beam energy equal to 400 and 2000 MeV. *low* corresponds to the efficiency of a pure silica fiber, *high* corresponds to the efficiency of a SPC fiber.

low noise, the Si diode S1227-33BR and the APD S5344 from Hamamatsu fit these requirements and their sensitivity (0.3 $A.W^{-1}$ for the diode and 20 $A.W^{-1}$ for the APD) have use to estimate the signal, note that the gain of the APD is set at 50 in the estimation and might be too high in some cases, saturation of the detector might perturb the measurement.

The expected signals as function of the wire position for both type of detectors are shown in Fig. 9 and Fig. 10

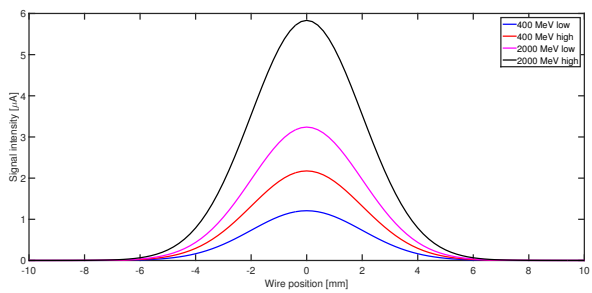

Figure 9: Expected signal at the output of the Si diode after 60 m of clear fiber.

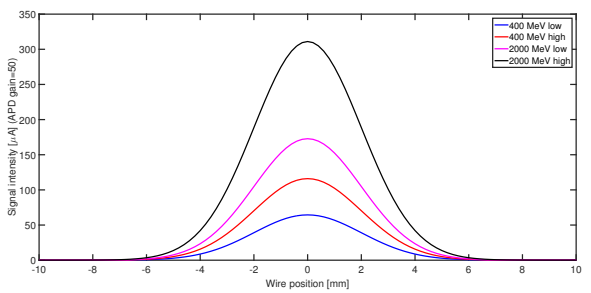

Figure 10: Expected signal at the output of the Si APD after 60 m of clear fiber.

The gain of the APD can be tuned, and at high energy a lower gain might be enough. At the time this paper is written, all these inputs are used has inputs for the FE specifications, after the preliminary design phase, the choice of the photodetector will be frozen.

Time Dependency of the Signal

A bunch by bunch measurement of the profile like in the synchrotron is not mandatory for a linac application, a time resolution of 0.5-1 μs is requested for the ESS WS system. The decay time of the detector assembly is long compare to the bunch frequency of the ESS linac (2.86 ns), the bunch structure will be vanished but some artifact might appear, simulations have been performed to cheek this effect.

In a first approximation, it was assumed that the bunch length (up to 20 ps) is null compare to the LSO crystal decay time, the charge per bunch is identical and the wire is not moving. The arrival time of the scintillation photon on the WLS fibber has been measured with the MC code, the decay time of the fiber and the different optical path of the shifted photon have been simulated in post processing for a single bunch. The time distribution obtained has been used to generate the time structure of the signal at the exit of the WLS fiber, by shifting the original distribution by 2.86 ns and adding the the new distribution to the previous distribution.

As shown in Fig. 11 for a beam pulse equal to 5 μs, the expected signal will have a rise and decay time equal to ≈300 ns, on the flat top on the signal the signal is almost constant (< 1 % peak to peak) and shows a time structure with a frequency equal to 352 MHz.

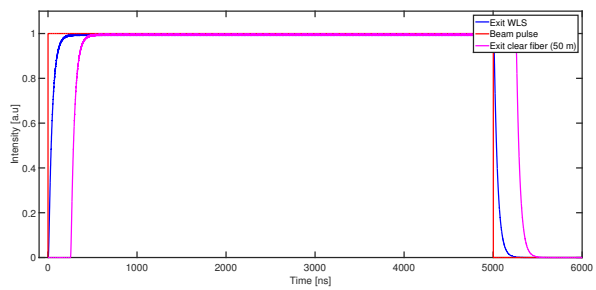

Figure 11: Expected rise/fall time signal for (i.e light) a single wire position, beam pulse is 5 μs.

After 50 meters of clear fiber, the signal will be shifted by 250 ns, it was assumed that the silica fibers are inducing time dispersion.

Detector Homogeneity

The homogeneity response of the detectors has been checked with same MC code, a pencil beam is moved across the beam pipe aperture form -25 mm to 25 mm in step of 5 mm, and then interacts with the tungsten foil, the energy deposited in each scintillators has been measured, it is assumed that the signal will be proportional to this quantity.

As shown in Fig. 12 , the signal can vary increase by almost 50 % across the beam pipe aperture if a single detector is installed. 4 detectors are needed to insure a good homogeneity. At 2000 MeV by summing the signal from the 4 detectors the absolute error is less than 2 % over the range considered in the study (see Fig. 13) , it has to be noted that the error is close to the statistical error of the MC code. At

ISBN 978-3-95450-178-6

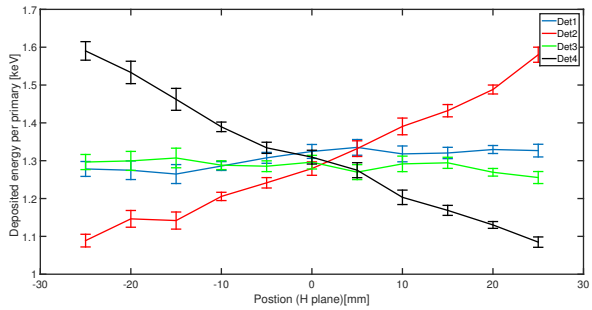

Figure 12: Energy deposited in each of the detectors at y=0 when the horizontal plane is scanned. Similar results are observed in the vertical plane with an inversion of the detector curves (i.e the flat curves are obtained with detector 2 and 4).

lower beam energy, the effect on the border will be higher, simulations are on going.

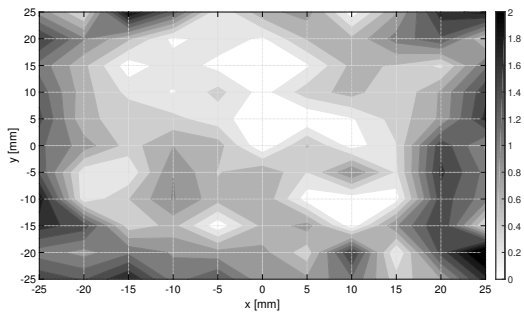

Figure 13: Absolute error map as function of the wire position, the beam energy is equal to 2000 MeV.

CONCLUSION AND OUTLOOK

The detector concept proposed in this paper seems interesting for the ESS application, in particular the absence of sensitive electronic in the tunnel area. The signal is expected to be less perturb by the interference of a high power accelerator environment (in particular the RF system), the conversion from light to current in the electronic cabinet will allow a cleaner signal.

Nevertheless, some assumptions taken during the study shall be confirmed, as mentioned in this paper the optical interfaces are almost perfect and the light trapping efficiency in the silica fiber to be evaluated, for this it is excepted to develop a small set-up in our laboratory. Prototypes might be down in order to asses this issues, in an ideal scenario, a beam test of few variants of the detector assembly shall be tested with beam, the goal will be to calibrate the MC simulations. In particular few reflective materials can be tested as well as different options for the optical coupling of the various part of the detector assembly. This phase will allow also to finalize the choice of the WLS fiber.

A full study of the Cherenkov detector will be also performed in the coming months.

REFERENCES

[1] M. Eshraqi et al., "The ESS linac", in *Proc. IPAC'14*, Dresden, Germany, THPME043, pp. 3320-3323.

[2] B. Cheymol, "ESS wire scanner conceptual design" ESS Technical note ESS-0020237.

[3] S. Filippov et al."Experimental Performance of SPD/PS Detector Prototypes" CERN-LHCb-2000-031.

[4] L. Zhang et al. "LSO/LYSO Crystals for Calorimeters in Future HEP Experiments" in *J. Phys.: Conf. Ser. 293 012004* 2011.

[5] A. Ferrari, P.R. Sala, A. Fasso, and J. Ranft, "FLUKA: a multi-particle transport code" CERN-2005-10 (2005), INFN/TC_05/11, SLAC-R-773.

[6] F. Duru et al."CMS Hadronic EndCap Calorimeter Upgrade studies for SLHC Cherenkov light collection from quartz plate" CMS note 2007/019 May 2007.

ISBN 978-3-95450-178-6